ECCOMAS Congress 2016
VII European Congress on Computational Methods in Applied Sciences and Engineering
M. Papadrakakis, V. Papadopoulos, G. Stefanou, V. Plevris (eds.)
Crete Island, Greece, 5–10 June 2016

A SIMPLE ANALYTICAL MODEL FOR THE ROCKING PREWEC SYSTEM

Dimitrios Kalliontzis[1] **and Sri Sritharan**[2]

[1] Ph.D. student in the Dept. of Civil, Environmental & Geo-Eng., Univ. of Minnesota-Twin Cities, Minneapolis 55455
kalli072@umn.edu

[2] Wilson Engineering Professor in the Dept. of Civil, Construction & Environmental Engineering, Iowa State University,
Ames, 50011
sri@iastate.edu

Keywords: Rocking, Concrete, Dynamics, Modelling, O-connectors, PreWEC

Abstract. *A simple analytical model for simulating a controlled rocking system consisting of a Precast Wall with End Columns (named as PreWEC) has been developed and compared against experimental results. The wall panel and end columns are secured to the foundation using prestressing, allowing PreWECs to experience rocking motions. The proposed model accounts for its predominant rotational degree of freedom formulation based on existing knowledge and adds new features to accurately capture the measured responses. They include a migrating rotation center that recognizes the variation in the contact length and its effect on the elongation in the post-tensioned tendons. Supplemental energy dissipation in PreWEC is provided by steel O-connectors, which horizontally join the wall panel to the end columns. These connectors are modelled using a system of nonlinear springs. Two different experiments were used to demonstrate the accuracy of the model validation, which include: a) a 5/18-scale PreWEC subjected to shake table motions; and b) a 1/5-scale PreWEC subjected to free vibration motions. It is shown that rotation responses and associated peaks experienced by the PreWEC rocking system can be accurately predicted using a simplified model.*

1 BACKGROUND

Rocking is a phenomenon that can influence the response of structures, which are allowed to uplift from their base. The eminent work by Housner [1] provided the fundamental knowledge and first steps towards modelling free rocking response of rigid members.

The topic of rocking response has received significant attention in recent years when vertical post-tensioning is introduced along the member length to control the rocking response and allow structural members to re-center upon removal of the lateral load [7, 10]. A simple form of a controlled rocking system is shown in **Fig. 1**, which shows the post-tensioning tendons anchored at the top of the member and the foundation. This concept has paved the way for developing new seismic resilient structural systems that are able to minimize both structural damage and residual drifts when subjected to earthquake input motions.

As part of the *NEES* Rocking Wall Project, a shake table testing of four controlled rocking concrete walls has been recently conducted by Nazari et al. [8] at 1/3.6 scale. As expected, the walls experienced negligible residual displacements and minimal damage that was mainly concentrated at wall compression toes. In another study, Ma [5] followed the original theory of Housner and extended it to modelling of controlled rocking systems as guided by experimental results from a rocking post-tensioned masonry wall. Ma observed from the experimental data that the assumption made in the Housner model of stationary pivot points at the bottom corners of the block did not hold for this controlled rocking unit. Instead, it was noted that the wall developed a contact over a finite area with the foundation surface, which was varying as a function of its angular displacement. This variation led to a continuously migrating rotation center residing within the contact area. The empirical model by Ma, therefore, accounted for this behavior by tracking the correct location of the pivot point. A method that provides a good estimate for the variation in the contact area of a controlled rocking body was suggested by Aaleti and Sritharan [1].

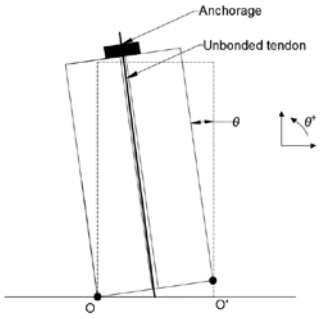

Figure 1: An idealized controlled rocking block.

2 RESEARCH SIGNIFICANCE

The focus of this paper is on modelling of a specific controlled rocking unit, as the PreWEC system. This system, shown schematically in **Fig. 2**, is one of the latest improvements in controlled rocking systems that incorporate supplemental hysteric damping. The PreWEC system consists of a precast wall with end columns with the wall panel and the end columns being individually anchored to the foundation using unbonded post-tensioned tendons [11]. The end columns are horizontally connected to the wall with mild steel O-connectors, which can be tailed to the strain and displacement demands [2]. This study presents analytical results from a model developed for the PreWEC system and compares them with experimental results obtained from shake table testing of PreWEC[1] [9] as well as from free vibration tests of another unit conducted by Twigden et al. [12].

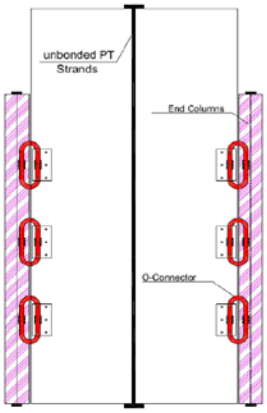

Figure 2: A schematic representation of the PreWEC System [9].

3 SUMMARY OF EXPERIMENTAL STUDIES

3.1 PreWEC system from *NEES* Rocking Wall Project

Test Setup

The unit designated as PreWEC[1] used twelve O-connectors and a wall specimen that was 1.524 mm long, 4,876.8 mm tall and 127 mm thick. The wall was post-tensioned to the foundation with five 270 Grade centrally placed steel strands. The total initial prestressing force applied through these strands was 865.18 kN.

The PreWEC[1] system was placed within a small pocket on top of the foundation with a layer of grout ensuring full contact between the prefabricated members. This unit was tested using a shake table, whose base was attached to the laboratory strong floor using tie-downs. A seismic mass consisting of a frame and two mass blocks (each block being 2,489.2 mm tall with a square cross-section of 1,219.2 x 1,219.2 mm^2) was used outside of the shake table, as shown in **Fig. 3**, connected to the wall panel using a rigid link beam.

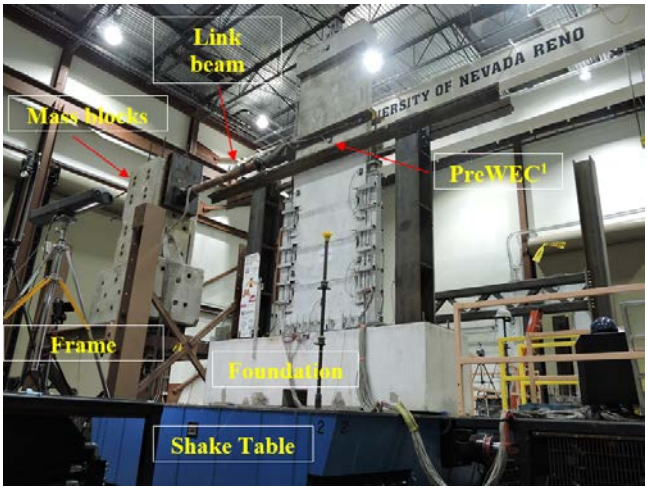

Figure 3: Test Setup for the PreWEC[1] [9].

Input Motions

The PreWEC[1] was subjected to a series of 42 test runs consisted of several input motions, including recorded earthquake excitations with varying intensities. Analysis of the PreWEC[1]

response in this study focused on the 23 first test runs, during which the O-connector experienced no deterioration or fracture. More information regarding the test setup, type of O-connectors, instrumentation and input motions are available on *NEEShub* by Nazari et al. [9].

3.2 PreWEC system tested by Twigden et al. [12]

Test Setup

The unit was 800 mm long, 3,000 mm high and 125 mm thick. The wall was anchored to the foundation with three steel strands of 15.2 mm diameter, each prestressed to $0.5\,f_{py}$. As shown in the test setup of **Fig 4**, this wall base was also placed in a grout pocket on the top of a foundation. Concrete mass blocks were placed on top of the wall to provide additional seismic mass. A lateral support frame was employed to minimize any out-of-plane motion of the system.

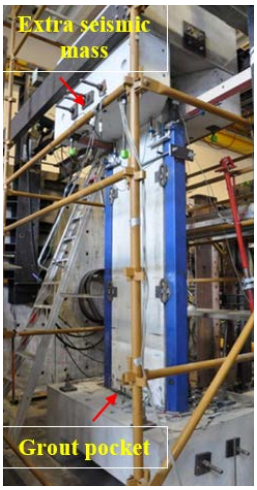

Figure 4: Test Setup for the PreWEC by Twigden et al. [10].

Input Motions

Two free vibration test runs were conducted on this specimen using: a) four (system designated as PreWEC-1); and b) six (system designated as PreWEC-2) O-connectors joining each end column with the wall panel. The specimen was tilted laterally using a hydraulic actuator and quickly released at the desired top lateral displacement level (i.e., 60 mm). More information about these experiments can be found in the paper by Twigden et al. [12], while information about the O-connectors used in this study can be found in Twigden and Henry [13].

4 MODELLING OF THE PREWEC SYSTEM

4.1 Equation of motion for PreWEC[1]

A dynamic system consisting of two generalized coordinates (q_1 and q_2) was built for simulating the response of PreWEC[1], where q_1 corresponds to the wall rotation and q_2 represents the rotation of the mass blocks with respect to the frame as observed from test videos. A schematic representation of this model is shown in **Fig. 5**. It is noted that the end columns were not included in this model and the contribution of O-connectors was included by assuming that the displacement demand imposed on the connectors was equal to the uplift of the wall panel

at one end and compression of the wall toes at the other end. This is consistent with experimental observations [11].

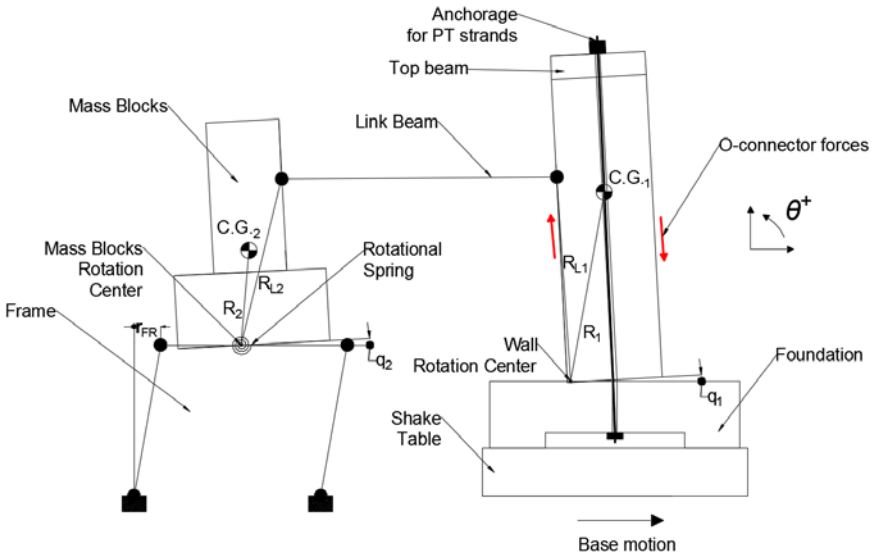

Figure 5: A schematic view of the model developed for PreWEC[1].

Modelling of the PreWEC[1] followed the Housner approach. However, the rotation center was assumed to be located in the middle of the wall contact length at the foundation interface and is, therefore, migrating as a function of the rotation q_1. The simplified method proposed by Aaleti and Sritharan [1] was employed to compute the expected contact length at 2% top lateral drift of the wall, assuming properties of confined concrete and an equivalent stress block at the wall toes. The variation of contact length from $0 \rightarrow 2\,\%$ drift was modified from the original method using the Meregotto-Pinto equation [6] as shown in **Fig. 6**.

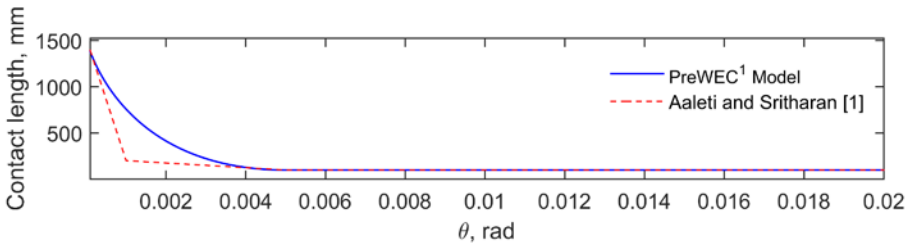

Figure 6: Contact length variation for PreWEC[1] model.

Similarly, the degree of freedom, q_2, corresponding to the mass concrete block rotation was modelled assuming an inverted pendulum, in which a linear rotational spring was used to capture the observed rotation of the mass blocks with respect to the supporting frame (see **Fig. 5**). The rotation center of the block was also modelled to vary as a function of its rotation in a similar fashion with **Fig. 6** with a minimum distance of 495 mm from its bottom corner being reached at $\theta = 0.005\,\text{rad}$.

In addition to the hysteric dissipation provided by the O-connectors, the system's energy dissipation included three damping components. As shown below, these components were provided by: a) the rocking wall panel; b) mass blocks; and c) frame supporting the mass blocks.

$$M_{damp,wall} = c_1 \dot{q}_1 \tag{1}$$

$$M_{damp,blocks} = c_2 \dot{q}_2 \tag{2}$$

$$F_{damp,\,frame} = sign\left(\dot{r}_{FR}\right) c_3 \sqrt{\left|\dot{r}_{FR}\right|} \tag{3}$$

where c_1, c_2 and c_3 were damping coefficients which were trained in an error minimization process using a set of two test runs (i.e., Test#4 and Test#18) [9]. Variables $M_{damp,wall}$ and $M_{damp,blocks}$ also served as numerical damping parameters in the numerical ODE solver.

Estimation of energy dissipation due to impact followed an approach described in Kalliontzis et al. [4]. Their proposed expression assume that the rotation centers of a rocking member just before and just after impact are as shown in **Fig. 7**. Using conservation of angular momentum before and after impact about the rotation center after impact, the equation for the coefficient of restitution (*COR*) in this approach is expressed as:

$$COR = \left[\frac{1 + \frac{MR^2}{I_{cm}} \left(1 - \left(\sin a\right)^2 \left(1 + k^2\right)\right)}{1 + \frac{MR^2}{I_{cm}} \left(1 - \left(\sin a\right)^2 \left(1 - k^2\right)\right)} \right]^2 \tag{4}$$

where k is a factor defining the location of rotation centers just before and just after impact; and I_{cm} denotes the mass moment of inertia of the block with respect to its gravitational center. With respect to Eq. 4, in the absense of a suitable value, $k = 0.72$ is recommended for concrete rocking members, which is used in this study.

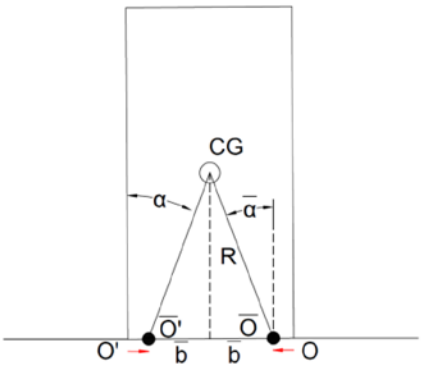

Figure 7: Rocking block with rotation centers $\bar{O}$ and $\bar{O}'$ just before and just after impact, respectively; where $\bar{b} = kb$ with $0 \le k \le 1$ and b is the block half-width [4].

Assuming the two rotational degrees of freedom shown in **Fig. 5** (i.e., one for the wall panel and the other for the mass blocks), two equations of motion were derived and they are presented in **Eqs. 5** and **6**.

$$\left(I_o + M_{EM}{L_{L_1}}^2 - \frac{{M_{EM}}^2}{\bar{I}_{o,b}}\left(L_{L_1}L_{L_2}\right)^2\right)\ddot{q}_1 = -{p_1}^2\left[\frac{\ddot{u}_g}{g}\cos\left(a_1 - |q_1|\right) + sign(q_1)\sin\left(a_1 - |q_1|\right)\right]$$
$$-sign(q_1)F_{PT}\left[\frac{W}{2} - \frac{C}{2}\right] - sign(q_1)\left[F_{down}\left(W - \frac{C}{2}\right) + F_{up}\frac{C}{2}\right] - M_{damp,wall} \quad (5)$$
$$-M_{EM}L_{L_1}\left(\ddot{u}_g + R_{L_1}\dot{q}_1^2\sin\left(a_{L,1} + q_1\right) + R_{L_2}\dot{q}_2^2\sin\left(a_{L,2} - q_2\right) + L_{L_2}\ddot{q}_{2,1}\right) - F_{damp,\,frame}L_{L_1}$$

$$\left(I_{o,b} + M_{EM}{L_{L_2}}^2\right)\ddot{q}_2 = -{p_2}^2 sign(q_2)\sin\left(a_2 - |q_2|\right) - M_{damp,blocks} - k_r q_2$$
$$-M_{EM}L_{L_2}\left(\ddot{u}_g + R_{L_1}\dot{q}_1^2\sin\left(a_{L,1} + q_1\right) + R_{L_2}\dot{q}_2^2\sin\left(a_{L,2} - q_2\right)\right) - F_{damp,\,frame}L_{L_2} \quad (6)$$
$$-M_{EM}\left(L_{L_1}L_{L_2}\right)\ddot{q}_1$$

with,

$$\ddot{q}_{2,1} = \frac{\begin{bmatrix} -{p_2}^2 sign(q_2)\sin\left(a_2 - |q_2|\right) - M_{damp,blocks} - k_r q_2 \\ -M_{EM}L_{L_2}\left(\ddot{u}_g + R_{L_1}\dot{q}_1^2\sin\left(a_{L,1} + q_1\right) + R_{L_2}\dot{q}_2^2\sin\left(a_{L,2} - q_2\right)\right) - F_{damp,\,frame}L_{L_2}\end{bmatrix}}{\left(I_{o,b} + M_{EM}{L_{L_2}}^2\right)} \quad (7)$$

$$L_{L_1} = -R_{L_1}\cos\left(a_{L,1} + q_1\right) \quad (8)$$

$$L_{L_2} = -R_{L_2}\cos\left(a_{L,2} - q_2\right) \quad (9)$$

$$p_1 = \sqrt{M_w g R_1} \quad (10)$$

$$p_2 = \sqrt{\frac{2}{3}M_{EM}gR_2} \quad (11)$$

$$\bar{I}_{o,b} = I_{o,b} + M_{EM}{L_{L_2}}^2 \quad (12)$$

In the above equations, $a_{L,1}$ and $a_{L,2}$ are the "slenderness" ratios with respect to the link beam location on the wall and mass blocks, respectively, which are updated with respect to the rotation center location; R_{L_1}, R_{L_2}, R_1 and R_2 are as identified in **Fig. 5**; F_{PT} represents the total force applied through the post-tensioned strands to the wall panel and it was estimated as per the Aaleti and Sritharan approach [1]; and F_{down} and F_{up} denote the O-connector forces, respectively, on the the uplift and compression sides of the wall panel due to the wall rotation.

In addition, the response of the wall system was also computed by using the experimentally recorded force applied through the link beam to the wall as the input parameter. In this case, the dynamic system consisted of a single degree of freedom, q_1, and its equation of motion is described in **Eq. 13**.

$$I_o\ddot{q}_1 = -{p_1}^2\left[\frac{\ddot{u}_g}{g}\cos\left(a_1 - |q_1|\right) + sign(q_1)\sin\left(a_1 - |q_1|\right)\right] - sign(q_1)F_{PT}\left[\frac{W}{2} - \frac{C}{2}\right]$$
$$-sign(q_1)\left[F_{down}\left(W - \frac{C}{2}\right) + F_{up}\frac{C}{2}\right] - M_{damp,wall} - F_{LinkBeam}L_{L_1} \quad (13)$$

where $F_{LinkBeam}$ represents the experimentally obtained link beam forces recorded using a load cell.

4.2 Modelling of O-connectors

Fig. 8a presents experimental data obtained from a quasi-static cyclic reversal test on the O-connector used in PreWEC[1] (Courtesy of Nazari Maryam, Ph. D. candidate at Iowa State University). Using a similar test setup to the one described by Henry et al. [2], the two pairs of O-connectors were subjected to the vertical displacement history shown in **Fig. 8b**.

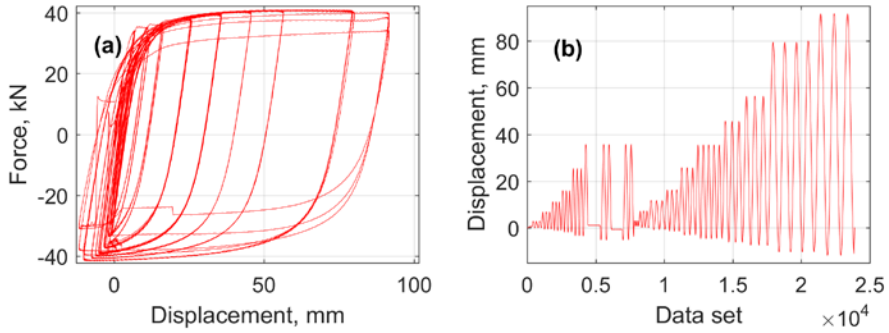

Figure 8: O-connector used in PreWEC[1] (a) measured force vs displacement response of one connector; and (b) applied displacement history protocol.

The recorded O-connector data was used to develop a numerical model for simulating the resistance of the connectors in the simulation of the PreWEC system. This model used the Meregotto-Pinto equation [6] to develop rules for the envelope, load reversals and reloading branches of the connector responses. **Fig. 9** compares model response with the experimental data, showing satisfactory agreement including the strength degradation experienced by the connector toward the end of testing.

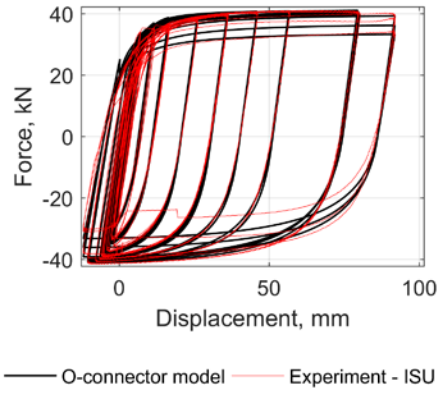

Figure 9: Comparison of force-displacement responses produced by the O-connector model and experimental data.

4.3 Initiation of rocking motion

Previous research studies that employed the Housner model for investigating free rocking motion routinely assumed that a free-standing rigid block is expected to uplift once the overturning moment produced by the ground acceleration exceeds the moment resistance of

the block, which depends on its mass and geometric properties. Considering the case of PreWEC[1], this limit is expressed as follows:

$$\frac{\ddot{u}_g}{g}+\frac{F_{LinkBeam}L_{L_1}}{Mgh}\geq\left[1+\frac{F_{PT,i}}{Mg}\right]\frac{b}{h} \tag{14}$$

with h representing the height of the gravity center of the system; and $F_{PT,i}$ is the initial post-tensioning force in the strands of the wall panel. While the above limit may accurately predict the initiation of controlled rocking of systems that can be reliably idealized as rigid blocks, its application to systems influenced by a migrating rotation center may not be satisfactory. Considering such a system at an initial rest condition being subjected to a horizontal ground motion, its imminent rotation point is unlikely to be located at its bottom corner. Hence, the moment equilibrium about this point is inapprorpiate without taking into account of the reaction forces at the wall base. To overcome this concern, the moment equilibrium may be taken about the correct rotation center, assuming that the rotation center coincides with the resultant compression force at the base.

Fig. 10 shows an example based on the PreWEC[1] model that the limiting expression in **Eq. 14** will not accurately capture when the rocking motion will initiate. The figure compares two analytical solutions established for the PreWEC[1] response assuming the aforementioned limit. The first case assumed a migrating rotation center during rocking motion as described in section 4.1, while the second case assumes that the rotation center is always located at one of the bottom wall corners (i.e., the wall is fully rigid). The corresponding experimental rotation time history is also plotted in the figure. It is seen that the two models fail to detect the beginning of rocking motion by approximately 2 seconds, while the first case predicts a significantly higher peak angular displacement response compared to the experimental observation. On the contrary, due to the higher moment resistance resulting from a fully rigid wall assumption, the second case significantly underestimates the peak displacement.

In order to tackle this issue associated with the initiation of rocking motion, the proposed model does not include a lower-bound limit for the overturning moment by assuming that the rotation center is located at the center of the wall base when the wall is at an initial rest mode. It is shown in the next section that this choice significantly contributes to accurately capturing the wall response for very small and large rotations.

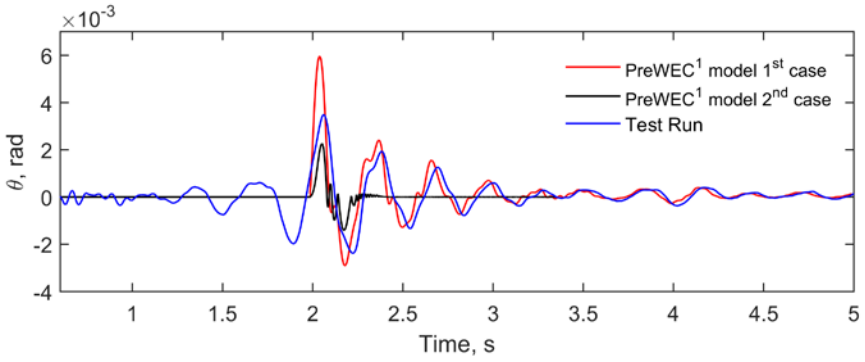

Figure 10: Measured rotation vs time of PreWEC[1] in the second input motion of Test#4 compared with analytical responses based on the limit of **Eq. 14**.

4.4 Modelling of PreWEC-1 and PreWEC-2 systems

Modelling of these systems followed the same approach as that described for PreWEC[1]. Variation of contact length in these systems was similarly estimated using the simplified

method proposed by Aaleti and Sritharan [1]. Moreover, these PreWECs used O-connectors with different dimensions and thus, the modelling rules were modified accordingly.

5 COMPARISON WITH EXPERIMENTAL RESPONSES

5.1 PreWEC[1] system

Fig. 11 presents several comparisons of PreWEC[1] model as per **Eq. 13**, with measured rotation time histories using $c_1 = 5I_o$. It is seen that the model is able to accurately reproduce the experimental responses for earthquake excitations of various intensities. Similar results were obtained with the use of the 2DOF system of **Eqs. 5-6** with suitable selections of the stiffness and damping parameters characterizing the seismic mass (i.e., $k_r = 39.63^5$ kN-mm; $c_2 = 6I_{o,b}$; $c_3 = 0.88$ kN$\sqrt{\text{s/mm}}$). These results are shown in Fig. 12.

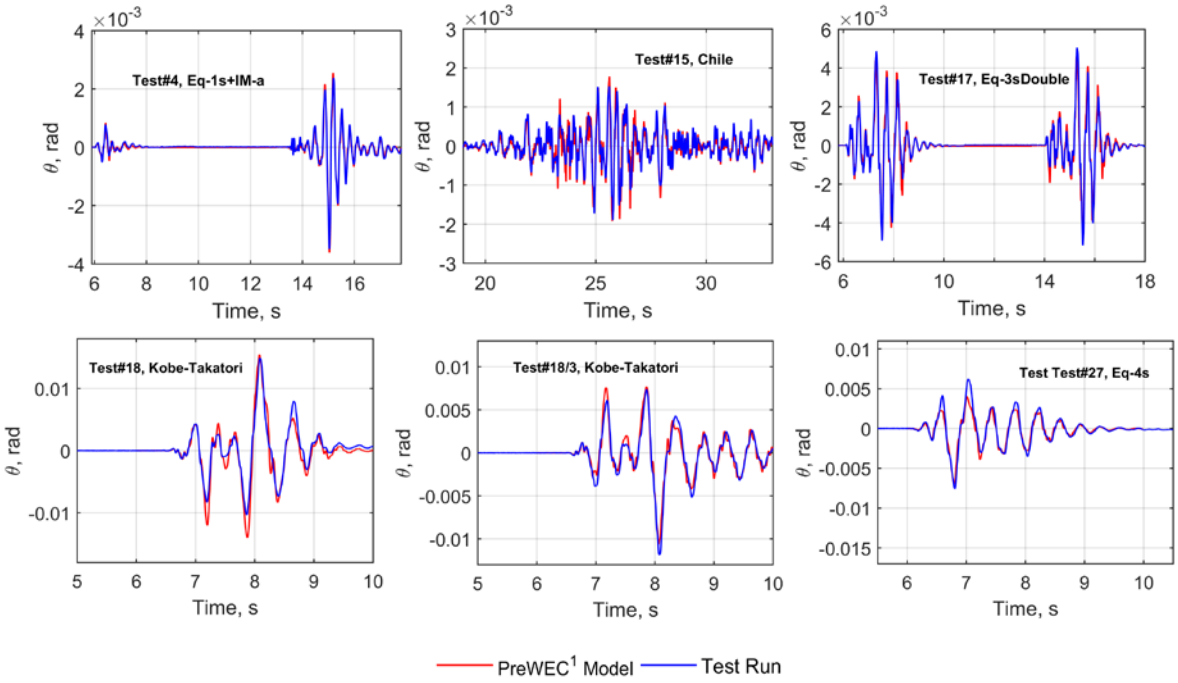

Figure 11: PreWEC[1] rotation time history responses from experimental and analytical results

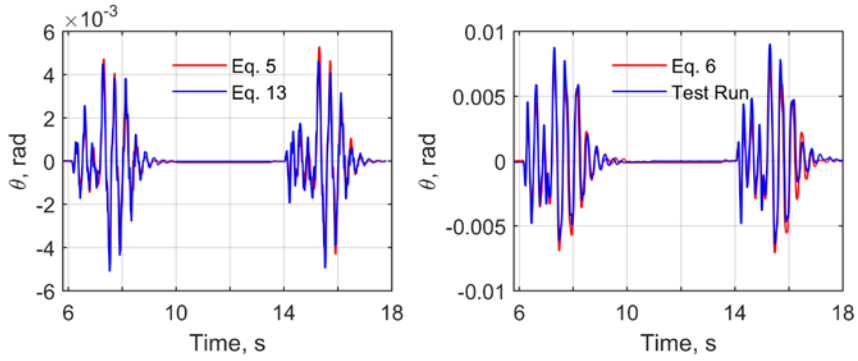

(a) (b)

Figure 12: Rotation time history responses of a) the PreWEC[1] using analytical results of **Eq. 5** and **Eq. 13**; and b) the mass blocks using analytical results of **Eq. 6** and experimental data (Test#17).

In **Fig. 13**, typical force-displacement responses are also presented for both the analytical and experimental data, showing that the numerical model can accurately follow the experimentally observed behavior.

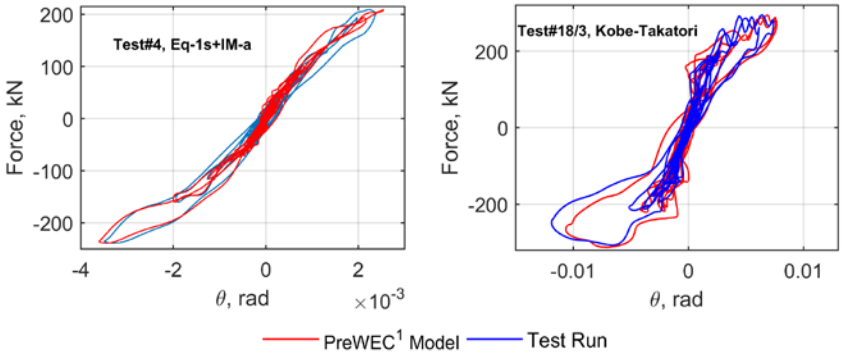

Figure 13: Comparison of force-displacement responses of the PreWEC[1] system

Finally, **Fig. 14** presents the error obtained between peak rotation responses as computed by the model of **Eq. 13** and experimental data, where positive values correspond to underestimation of the peaks while the negative peaks reflect overestimation of the peak responses. It is seen that the model is able to accurately capture the maximum responses established from the shake table tests, while the measured error remains below 10% for most of the cases. A mean value computed from all the absolute error measures was found to be approximately 5%.

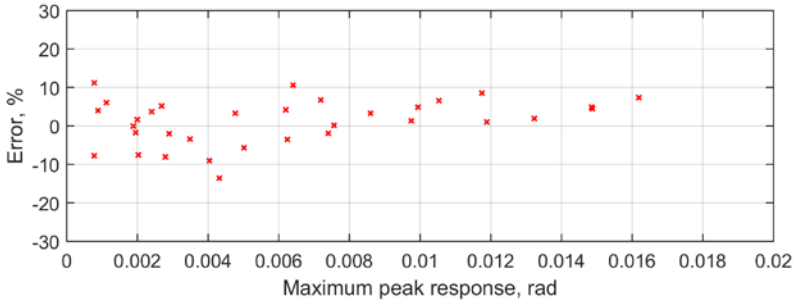

Figure 14: Estimated error for the maximum peak responses predicted by the analytical model

5.2 PreWEC-1/2 systems

Fig. 15 presents the analytical solutions for the free vibration motion of these PreWECs conducted by the model of **Eq. 13** (where $F_{LinkBeam} = 0$ and $\ddot{u}_g = 0$) using a) four, and b) six O-connectors. Note that a value of $c_1 = 2.5I_o$ was selected in this case. Also included in this figure are experimentally recorded responses. For both cases, the free vibration responses closely match measured responses.

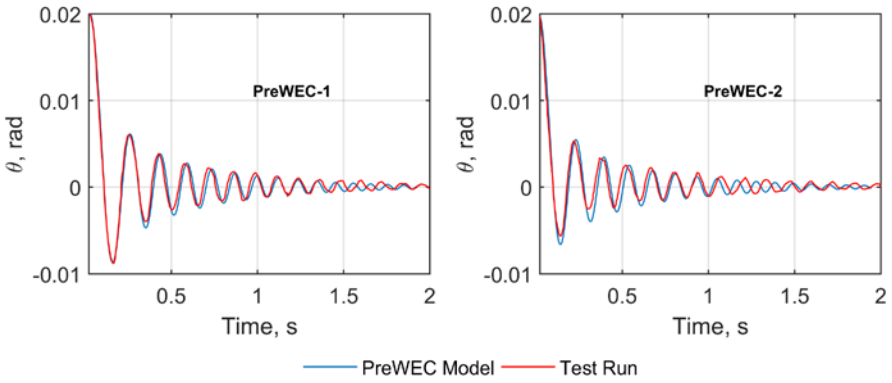

Figure 15: PreWEC-1 and PreWEC-2 Models vs experimental results of free vibration tests.

6 CONCLUSIONS

An analytical approach for estimating the dynamic response of PreWEC systems is introduced in this paper. The proposed method uses the Housner's model as the basis for developing the equation of motion, while allowing a migrating rotation center that was defined based on the contact length-rotation relationship by the Aaleti and Sritharan method [1]. Energy dissipation in the proposed model consisted of a) an impact mechanism that was expressed per the Kalliontzis et al. approach [4], b) hysteric dissipation provided by the O-connectors, and c) empirically selected continuous damping mechanisms, which additionally served as numerical damping parameters for solving the equation of motion.

Validation of the analytical model used two independent experimental investigations conducted using: a) shake table, and b) free vibration testing. Comparison with these experimental results show that the model developed for the PreWEC with hysteric energy dissipation is appropriate for both cases.

7 ACKNOWLEDGEMENTS

The work presented in the paper was undertaken as part of the "*NEES* Rocking Wall" Project with funding from the National Science Foundation (NSF) under Grant No. 1041650. The authors would like to thank Maryam Nazari, Ph.D. candidate and Lin Shibin, Postdoctoral Research Associate, both at Iowa State University, for their help with the experimental data analyses. Any opinions, findings and conclusions or recommendations expressed in this material are those of the authors and do not necessarily reflect the views of NSF.

REFERENCES

[1] S. Aaleti, S. Sritharan, A simplified analysis method for characterizing unbonded post-tensioned precast wall systems. *Engineering Structures*, **31**(12), 2966-2975, 2009.

[2] Henry R. S., S. Aaleti, S. Sritharan, J. M. Ingham, Concept and finite-element modelling of new steel shear connectors for self-centering wall systems. *J. Engineering Mechanics*, ASCE, **136**(2), 220-229, 2010.

[3] G. W. Housner, The behaviour of inverted pendulum structures during earthquakes. *Bull. Seismol. Soc. Am.*, **53**(2), 403-417, 1963.

[4] D. Kalliontzis, S. Sritharan, A. Schultz, Modified coefficient of restitution model for free rocking members. *J. Struct. Eng.*, ASCE, under review.

[5] Q. T. M. Ma, The mechanics of rocking structures subjected to ground motion. *PhD Thesis*, The University of Auckland, New Zealand, 2009.

[6] M. Meregotto, P. Pinto, Method of analysis for cyclically loaded reinforced concrete plane frames including changes in geometry and nonelastic behaviour of elements under combined normal force and bending, *Proc. Symp. Resistance Ultim. Deformability Struct. Acted Well-defined Repeated Loads*, IASBE, Lisbon, Portugal, 1973.

[7] S. D. Nakaki, J. F. Stanton, S. Sritharan, An overview of the PRESSS five-story precast test building, *PCI J.*, March-April, 1999.

[8] M. Nazari, S. Aaleti, S. Sritharan, Shake table testing of unbonded post-tensioned precast concrete walls. *10th U.S. National Conf. Earthquake Eng.*, Alaska, 2014.

[9] M. Nazari, S. Aaleti, S. Sritharan, Shake table testing of single rocking wall 1 (SRW1) @ UNR. *Network for Earthquake Eng. Simulation (distributor)*, DOI: 10.4231/D3D29P75Z, 2015.

[10] M J N Priestley, S Sritharan, J R Conley, S Pampanin, Preliminary results and conclusions from the PRESSS five-story precast concrete test bulding. *PCI J.*, **44**(6), 42-67, 1999.

[11] S. Sritharan, S. Aaleti, R. H. Henry, K. Y. Liu, K. C. Tsai, Precast concrete wall with end columns (PreWEC) for earthquake resistant design. *Earthquake Eng. Struct. Dyn.*, published online, 2015.

[12] K. M. Twigden, R. S. Henry, Q. T. Ma, Pseudo-static cyclic, snap back and shake table testing of PreWEC self-centering wall systems. *10th U.S. National Conf. Earthquake Eng.*, Alaska, 2014.

[13] K. M. Twigden, R. S. Henry, Experimental response and design of O-connectors for rocking wall systems. *Structures*, **3**, 261-271, 2015.